# Combined design and control optimization of hybrid vehicles

Nikolce Murgovski[1,a], Xiaosong Hu[a], Lars Johannesson[a,b], Bo Egardt[a]

[a] *Department of Signals and Systems, Charmers University of Technology, SE-41 296 Gothenburg, Sweden*
[b] *Viktoria Swedish ICT, SE-41 756 Gothenburg, Sweden*

## Abstract

Hybrid vehicles play an important role in reducing energy consumption and pollutant emissions of ground transportation. The increased mechatronic system complexity, however, results in a heavy challenge for efficient component sizing and power coordination among multiple power sources. This chapter presents a convex programming framework for the combined design and control optimization of hybrid vehicles. An instructive and straightforward case study of design and energy control optimization for a fuel cell/supercapacitor hybrid bus is delineated to demonstrate the effectiveness and the computational advantage of the convex programming methodology. Convex modeling of key components in the fuel cell/supercapactior hybrid powertrain is introduced, while a pseudo code in CVX is also provided to elucidate how to practically implement the convex optimization. The generalization, applicability, and validity of the convex optimization framework

*Email addresses:* nikolce.murgovski@chalmers.se (Nikolce Murgovski), xiaosong@chalmers.se (Xiaosong Hu), larsjo@chalmers.se, lars.johannesson@viktoria.se (Lars Johannesson), bo.egardt@chalmers.se (Bo Egardt)

[1] Corresponding author, Tel: +46 31 7724800, Fax: +46 31 7721748

are also discussed for various powertrain configurations (i.e., series, parallel, and series-parallel), different energy storage systems (e.g., battery, supercapacitor, and dual buffer), and advanced vehicular design and controller synthesis accounting for the battery thermal and aging conditions. The proposed methodology is an efficient tool that is valuable for researchers and engineers in the area of hybrid vehicles to address realistic optimal control problems.

*Keywords:* Hybrid Electric Vehicle, Component Sizing, Energy Management, Convex Optimization, Optimal Control, Fuel Cell, Energy Storage System

---

## 1. Introduction

Rising fuel prices and the risk of global warming has stimulated development towards increasingly energy efficient vehicles. This ongoing development has led to improved energy efficiency of combustion engines, and reduced aerodynamic drag and rolling resistance due to more streamlined vehicle design and improved tires.

In addition to engine efficiency, aerodynamic drag and rolling friction, the two main contributors to the overall losses in a vehicle are braking losses and engine idling losses. Hybrid vehicles reduce these losses by including an energy buffer in the powertrain, making it possible to regenerate braking energy and turn off the engine at part load. For a detailed overview on hybrid vehicles, see e.g. Guzzella and Sciarretta (2013).

Besides stimulating the development towards increasingly energy efficient vehicles, the rising fuel prices and the risk of global warming has led to

an increased interest for electrification of road transport. Electrified vehicles are being introduced to the market, such as Hybrid Electric Vehicles (HEVs), Plug-in Hybrid Electric Vehicles (PHEVs), and pure Electric Vehicles (EVs). An example is a PHEV public transportation system that uses electric charging infrastructure installed along densely trafficked city bus lines (Volvo Group, 2013; TOSA, 2013). The PHEV public transportation system thus offers a flexible crossbreed between an HEV city bus and a trolley-bus. In Volvo Group (2013), the PHEV city bus is equipped with a high-energy battery that is charged at the beginning of the bus line, whereas the bus in TOSA (2013) is equipped with a high-power battery that is charged with very high power at several supercapacitor docking stations along the bus line. The high power charging allows the bus to drive a significant part of the bus line electrically, even though the charging infrastructure might be sparsely distributed and charging durations might be short.

The development of increasingly energy efficient vehicles and the electrification of road transport mean that the world is on the verge of a change in both commercial and personal transportation. This global change brings significant industrial challenges, as well as new business opportunities for the manufactures that lead the development. However, the development of new technology requires substantial investments. It is therefore crucial to assess the competitiveness of a new vehicle concept early on in the development process.

Assessing the potential of a hybrid vehicle is not trivial. This is due to increased complexity of hybrid powertrains, and the complex interplay between electrified vehicles and the charging infrastructure. Moreover, when

assessing hybrid vehicles the energy efficiency depends on how well adapted the energy/power management controller is to driving conditions (Johannesson et al., 2009; Larsson et al., 2012; Sciarretta and Guzzella, 2007). In (P)HEVs the energy management controller interprets the pedal position as a torque/power demand that is to be delivered from the powertrain, and decides the operating point of the primary power unit, e.g. combustion engine or fuel cell system. As a consequence, the controller decides the rate of charge/discharge of the energy buffer. In a simulation study that evaluates a hybrid powertrain concept, a badly tuned energy management control may lead to wrong conclusions and potentially bad investments (Sundström et al., 2010; Murgovski et al., 2012c; Hu et al., 2013). It is therefore of high interest to develop software for simulation studies of hybrid vehicles that can find the best powertrain configuration and simultaneously tune/design the energy management controller. These tools need to be computationally efficient to assess many possible variants, which arise when studying the interplay between the powertrain and the infrastructure for different combinations of price scenarios for fuel, infrastructure and powertrain components.

The problem of combined plant design and control optimization can be approached in different ways. Typically, the problem is handled by decoupling the plant and controller, and then optimizing them sequentially or iteratively (Assanis et al., 1999; Galdi et al., 2001; Wu et al., 2011; Fathy et al., 2004; Peters et al., 2013). A well known iterative procedure formulates the optimization problem as a bi-level program, i.e., an optimization problem constrained by a collection of other interrelated optimization problems (Conejo et al., 2006; Mnguez et al., 2013). Bi-level programs are non-convex

by nature, but at certain cases they can be solved within satisfactory accuracy (Bertsekas and Sandell, 1982). However, sequential and iterative strategies generally fail to achieve global optimality (Reyer and Papalambros, 2002). An alternative is a nested optimization strategy, where an outer loop optimizes system's objective over the set of feasible plants, and an inner loop generates optimal controls for plants chosen by the outer loop (Fathy et al., 2004). This approach delivers the globally optimal solution, but it may induce heavy computational burden (when, e.g., dynamic programming is used to optimize the energy management), or may require substantial modeling approximations (Filipi et al., 2004; Kim and Peng, 2007; Sundström et al., 2010). High computational efficiency could be achieved, if the plant design and control are optimized simultaneously, by, e.g., formulating and solving the problem as a convex program (Boyd and Vandenberghe, 2004).

This chapter addresses the need for an efficient software tool by giving a tutorial on how to formulate the (P)HEV assessment and powertrain sizing problem as a convex optimization problem. The key element in the convex optimization framework is to find modeling approximations and relaxations that allow the convex optimization techniques and convex solvers to be applied. The convex problems can be solved efficiently using standard convex optimization solvers and high level optimization modelling languages, such as CVX (Grant and Boyd, 2010) and YALMIP (Löfberg, 2004).

The application of convex optimization to hybrid powertrain energy management control has been known for some time (Tate and Boyd, 2000; Back et al., 2002; Terwen et al., 2004; Koot et al., 2005; Beck et al., 1997). In these articles, convex optimization was used to compute the optimal energy

management control, either over an entire driving cycle, or in a receding horizon predictive control over a limited time horizon. A more recent development is the use of convex optimization to solve the combined problem of simultaneous optimization of energy management and component sizing (Murgovski et al., 2011, 2012c). The short computational time of this method requires limited computational resources for detailed investigations of a wide range of price-case scenarios for fuel, electricity, charging infrastructure and powertrain components.

The tutorial presented in this chapter is centered on a case study of a fuel cell hybrid city bus which uses a supercapacitor as energy buffer. The purpose of the example is to introduce the main modelling assumptions required to formulate the powertrain assessment and sizing problem as a convex optimization problem. The code example is presented both as a CVX pseudo code (Grant and Boyd, 2010) and a complete, publicly accessible Matlab code (Murgovski, 2014).

The chapter is organized as follows. The case study for the fuel cell hybrid bus is presented in Section 2. Section 3 describes how to generalize the convex optimization framework to various powertrain configurations, different energy storage systems, and advanced vehicular design and controller synthesis accounting for battery thermal and aging conditions. The chapter is ended with a conclusion.

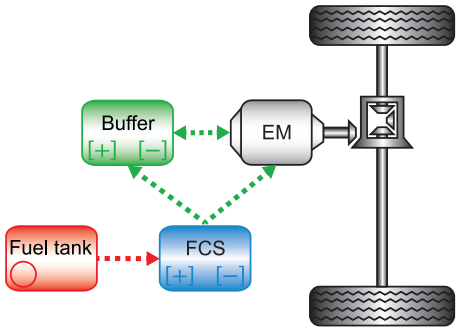


Figure 1: Fuel cell hybrid powertrain. The vehicle is propelled by an electric machine (EM), which obtains energy from a fuel cell system (FCS), or an electric buffer (battery or supercapacitor). When EM operates as a generator, mechanical energy from the wheels is converted to (and stored as) electrical energy in the buffer.

## 2. Case study: optimal control and sizing of a fuel cell hybrid vehicle

In order to show utilization of convex optimization, this section considers the optimization problem of sizing a hybrid city bus. The bus is driven by an electric machine that obtains electrical energy from a fuel cell system (FCS) and an electric buffer, as illustrated in Figure 1.

Fuel cells allow direct conversion of chemical energy to electrical energy. This has several advantages compared to ICE driven vehicles. Vehicles equipped with fuel cells have higher well-to-wheel efficiency, lower noise emission, and lower (or zero) environmental pollution (Xu et al., 2009; Eberle et al., 2012). Additionally, a fuel cell vehicle hybridized with an electric buffer, typically a battery or a supercapacitor, may further improve vehicle's energy efficiency. This can be achieved by 1) recuperating braking energy that can be stored in the buffer for a later use, and 2) allowing the FCS

to operate at higher efficiency by carefully splitting demanded power between the FCS and the electric buffer. Furthermore, fuel cell hybrid vehicles (FCHVs) may allow 1) reduction in weight and cost by downsizing the FCS, 2) prolonged lifetime of the FCS, 3) faster dynamic response of the vehicle, 4) shorter warm-up time (Feroldi et al., 2009). FCHVs, however, are more complicated than non-hybrid vehicles. Hence, the problem of sizing an FCHV powertrain, to be introduced in the following section, is non-trivial.

### *2.1. The problem of sizing an FCHV powertrain*

City busses are considered an interesting application of vehicle hybridization, due to the high potential for improvement in fuel economy (Murgovski, 2012). In this example a fuel cell hybrid electric bus is studied, which uses hydrogen as a chemical fuel, and supercapacitor pack as an electric buffer. The bus follows a certain time schedule and velocity/acceleration trajectory in order to comply with traffic limitations, passengers' comfort requirements and driveability. Then, a bus line can be described by the desired velocity profile, road altitude, and information about average stand-still intervals at bus stops or traffic stops. An example of a bus line is depicted in Figure 2, where the bus starts and ends the route at zero speed and equal altitude, thus conserving vehicle's kinetic and potential energy. Furthermore, to purely study operational efficiency of the city bus, it is also required that buffer energy at the final time is equal to the initial amount of energy. Then, the operational cost of this vehicle depends solely on the quantity of hydrogen consumed along the bus line.

Operational cost of the vehicle can be minimized by using predictive information of the known bus line. The goal is to optimally split demanded

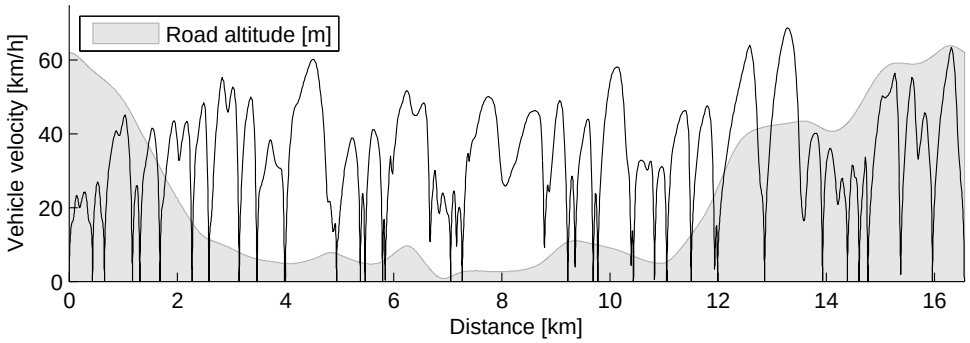


Figure 2: Model of a bus line, expressed by demanded vehicle velocity and road altitude. The initial and final velocities and road altitudes, respectively, are equal, thus conserving kinetic and potential energy of the vehicle.

power between the FCS and the supercapacitor, without violating system constraint. This requires higher utilization of supercapacitor energy, making it beneficial to increase supercapacitor size, both for increased freedom of FCS operation, and higher recuperation of braking energy. However, a larger buffer, in terms of power rating and energy capacity, increases the component cost of the vehicle. Then, to keep component cost down, the possibility of downsizing the FCS is also considered, such that the optimal tradeoff is reached between component cost and operational cost within the lifetime of the vehicle. This is a multi-objective optimization problem where two objectives are weighted, i.e. operational and component cost. The optimization framework for solving this problem is illustrated in Figure 3, while a verbal formulation is provided in Table 1. The mathematical description of the optimization problem is resumed in Section 2.2.6, after modeling details of the FCHV powertrain are provided.

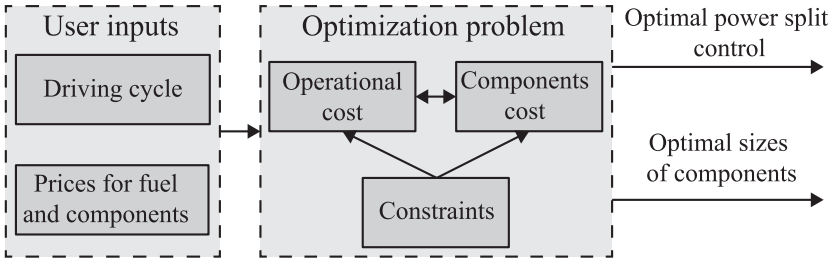


Figure 3: Optimization framework for simultaneous component sizing and energy management of a hybrid city bus. After user inputs are provided, the combined operational and components cost are minimized simultaneously, in order to obtain the optimal power split control and sizes of powertrain components.

### *2.2. Mathematical model of the powertrain sizing problem*

The problem formulated in Table 1 is revisited here, by providing mathematical meaning to constraints and the objective function. To the end of this section it will be shown that the powertrain sizing problem can be formulated as a convex optimization problem.

#### *2.2.1. Longitudinal vehicle dynamics*

The vehicle is assumed a point mass system, where the vehicle mass $m(s_F, s_B)$ depends on sizing variables $s_F$ and $s_B$, denoting scaling factors for the fuel cell system and the electric buffer. The longitudinal dynamics of the point mass system can be described by the torque demanded on the shaft between the electric machine and the final (differential) gear,

$$\begin{aligned} T_{dem}(s_F, s_B, t) = &\left( J_V + m(s_F, s_B)\frac{R_w^2}{r_{fg}^2} \right) \dot{\omega}_M(t) + \frac{\rho_{air} A_f c_d R_w^3}{2 r_{fg}^3} \omega_M^2(t) \\ &+ m(s_F, s_B)\frac{c_r R_w}{r_{fg}} g \cos\alpha(t) + m(s_F, s_B)\frac{R_w}{r_{fg}} g \sin\alpha(t), \end{aligned} \tag{1}$$

Table 1: Optimization problem for simultaneous component sizing and energy management of a hybrid city bus.

| |
|---|
| Minimize: |
| Operational + component cost; |
| Subject to: |
| Driving cycle constraints, |
| Energy conversion and balance constraints, |
| Buffer dynamics, |
| Physical limits of components, |
| ... |
| *(For all time instances along the bus line).* |

where $\omega_M(t)$ is speed of the electric machine, $J_V$ is vehicle's rotational inertia, which includes the inertia of the wheels, the electric machine, the final gear, the drive axels and all rotating shafts. The EM speed is directly related to the demanded velocity of the bus line

$$\omega_M(t) = v_{dem}(t)\frac{r_{fg}}{R_w}, \tag{2}$$

where $r_{fg}$ is gear ratio of the final gear and $R_w$ is wheels radius. The demanded torque in (1) is a sum of four contributions: 1) acceleration torque, 2) retarding torque due to aerodynamic drag, 3) retarding torque due to rolling resistance with the road, and 4) gravitational torque due to road inclination $\alpha(t)$. Description of the coefficients and their values used in the example are given in Table 2.

The vehicle mass consists of a constant part, and part varying linearly

Table 2: Vehicle parameters and corresponding values used in the optimization example.

| Parameter | Value |
|---|---|
| Vehicle's rotational inertia | $J_V = 55\,\mathrm{kgm}^2$ |
| Vehicle's baseline mass | $m_0 = 14\,573\,\mathrm{kg}$ |
| FCS's baseline mass | $m_F = 223\,\mathrm{kg}$ |
| Buffer's baseline mass | $m_B = 176\,\mathrm{kg}$ |
| Wheels' radius | $R_w = 0.509\,\mathrm{m}$ |
| Final gear ratio | $r_{fg} = 4.7$ |
| Vehicle's frontal area | $A_f = 7.54\,\mathrm{m}^2$ |
| Aerodynamic drag coefficient | $c_d = 0.7$ |
| Rolling resistance coefficient | $c_r = 0.007$ |
| Air density | $\rho_a = 1.184\,\mathrm{kg/m}^3$ |
| Gravitational acceleration | $g = 9.81\,\mathrm{m/s}^2$ |

with the scaling factors of the fuel cell system and the electric buffer,

$$m(s_F, s_B) = m_0 + m_F s_F + m_B s_B. \tag{3}$$

A constant baseline vehicle mass $m_0$ is considered and it is assumed that the final gear is lossless. The assumptions are only for didactic reasons, to keep the problem relatively simple. It is, of course, possible to vary vehicle mass with time, in case the typical number of on-board passengers between bus stops is known. Other possibilities, such as maximizing payload, or using a more detailed powertrain models, could be included without infringing problem convexity. Further details on this topic can be found in Murgovski et al. (2012c).

Using (3) in (1) allows the demanded torque to be written as

$$T_{dem}(s_F, s_B, t) = T_0(t) + T_1(t)s_F + T_2(t)s_B, \tag{4}$$

where it is evident that the torque is an affine function of the scaling coefficients $s_F$ and $s_B$. Furthermore, a common practise when deciding control strategies, or comparing different vehicle concepts, is to assume that the vehicle exactly follows the driving cycle (Guzzella and Sciarretta, 2013). The vehicle model is then an inverse simulation model, in which the traction torque of the powertrain is considered equal to the demanded torque of the driving cycle. This reduces the computational burden in simulations by removing the driver model and the vehicle velocity from the state vector (Sciarretta and Guzzella, 2007). Instead, the full knowledge of the driving cycle is employed, considering that $v_{dem}(t)$ and $\dot{v}_{dem}(t)$ are known at each time instant. Hence, the vectors $\omega_M(t)$, $T_0(t)$, $T_1(t)$ and $T_2(t)$ in (2) and (4) are also known at each point of time, and the only unknown variables in (4) are the scaling coefficients $s_F$ and $s_B$.

*2.2.2. Electric machine*

The FCHV powertrain delivers the demanded torque in (4) by the electric machine, which is powered by the fuel cell system and the electric buffer. The EM is also used to recuperate braking torque and store the energy in the buffer. These processes can be mathematically described by mechanical and electrical torque/power balance constraints

$$T_M(t) = T_0(t) + T_1(t)s_F + T_2(t)s_B + T_{brk}(t), \tag{5}$$

$$P_{Me}(\cdot) = P_{Fe}(t) + P_B(t) - P_{Bd}(\cdot) - P_a, \tag{6}$$

where $T_M(t)$ and $P_{Me}(\cdot)$ are torque and electrical power of the electric machine, $T_{brk}(t)$ is torque dissipated due to friction braking, $P_a = 7\,\text{kW}$ is power consumed by auxiliary devices. The powers $P_{Fe}(t)$, $P_B(t)$ and $P_{Bd}(\cdot)$ denote electrical power of the FCS, internal and dissipative power of the buffer, respectively, and will be detailed later in Section 2.2.3 and Section 2.2.4. The notation $f(\cdot)$ is a compact notation that indicates a function of optimization variables. These functions will be detailed later, after the needed models are presented.

The relation between electrical and mechanical EM power are represented by a static model, illustrated in Figure 4. It can be observed in Figure 4(b)

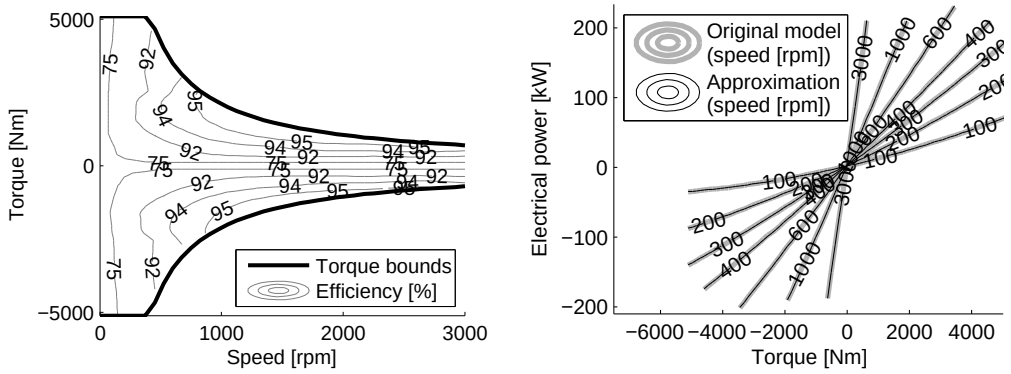


(a) Original model.

(b) Approximated model.

Figure 4: Quasi-static model of an electric machine and its corresponding approximated model. The electrical power of the approximated model is quadratic in torque within the operating speed range of the electric machine.

that the electric power appears convex in torque, for speed measurements within the operating speed range of the EM. Figure 4(b) also illustrates an

approximated model, quadratic in torque,

$$P_{Me}(T_M(t), t) = a_0(\omega_M(t)) + a_1(\omega_M(t))T_M(t) + a_2(\omega_M(t))T_M^2(t), \quad (7)$$

with coefficients parameterized in speed. The approximation is performed over a grid of EM speeds, and the coefficients, $a_j, j = 0, 1, 2$, are computed at each time instant using linear interpolation at the known EM speeds $\omega_M(t)$. The coefficients $a_2(\omega_M(t))$ are nonnegative, which ensures that $P_{Me}(\cdot)$ is convex in $T_M(t)$. Besides using it in this example, the quadratic model has been widely used in literature for both electric machines and internal combustion engines. For further reading on validity of this model, see Guzzella and Sciarretta (2013) and references therein.

The machine generating torque is constrained by a torque limit

$$T_M(t) \geq T_{Mmin}(\omega_M(t)), \quad (8)$$

which is also a function of EM speed. Constraints can be imposed on the machine motoring torque and maximum operating speed, but an explicit notation is omitted here, assuming that these constraint will not be violated. This is a natural assumption, as otherwise the problem will be infeasible and there will be no need for optimization. An illustration of the EM torque limits is given in Figure 4(a).

*2.2.3. Fuel cell system (FCS)*

The fuel cell system (FCS) consists of fuel cells connected in series, and auxiliary systems, such as hydrogen storage and supply system, air supply system, water management system, and cooling system. The FCS produces DC electricity via electrochemical reactions, where efficiency depends on electrical power, as illustrated in Figure 5(a). The fuel power of the baseline

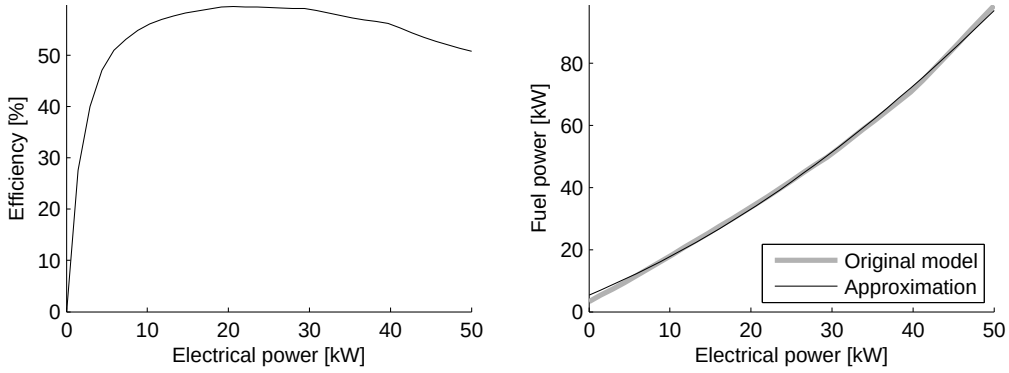


(a) Original model. (b) Approximated model.

Figure 5: Quasi-static model of the baseline fuel cell system and its corresponding approximated model. The fuel power of the approximated model is quadratic in electrical power.

(non-scaled) FCS can be approximated as

$$P_{FfB}(\cdot) = b_0 + b_1 P_{FeB}(t) + b_2 P_{FeB}^2(t) \tag{9}$$

with $b_2 \geq 0$. A comparison between the original and approximated baseline FCS is illustrated in Figure 5(b).

A quadratic FCS model has also been used in Tazelaar et al. (2012a,b), while a more detailed description and experimental validation has been performed by Funck (2003) and Gasser (2005). It has also been indicated by Tazelaar et al. (2012a,b); Funck (2003); Gasser (2005) that both the FCS fuel power and electrical power scale linearly with size, by, e.g. adding or removing cells to the stack. Hence, by denoting $P_{Ff}(t) = s_F P_{FfB}(t)$, $P_{Fe}(t) = s_F P_{FeB}(t)$, the fuel power of the scaled model can be expressed as

$$P_{Ff}(P_{Fe}(t), s_F) = b_0 s_F + b_1 P_{Fe}(t) + b_2 \frac{P_{Fe}^2(t)}{s_F}. \tag{10}$$

This function is convex in $s_F$ and $P_{Fe}(t)$, for any positive scaling factor $s_F$.

A constraint is imposed on the electrical power

$$0 \leq P_{Fe}(t) \leq s_f P_{FeBmax} \tag{11}$$

where $P_{FeBmax}$ is rated power of the baseline FCS.

*2.2.4. Supercapacitor*

The supercapacitor pack is built of $n_0$ identical cells described by an open circuit voltage $u(t)$ connected in series to an internal resistance $R$. The arrangement of cells in series/parallel is irrelevant, because the pack energy and power depends only on the total number of cells. The pack dissipative power is described by

$$P_{Bd}(\cdot) = Ri^2(t)n_0 \tag{12}$$

where $i(t)$ denotes cell current. An alternative expression, in terms of internal pack power $P_B(t)$ and pack energy $E_B(t)$, is

$$P_{Bd}(P_B(t), E_B(t)) = \frac{RC}{2}\frac{P_B^2(t)}{E_B(t)}, \tag{13}$$

which is a convex function of $P_B(t)$ and $E_B(t)$. The pack energy, $E_B(t) = Cu^2(t)n_0/2$, is considered positive, i.e.

$$E_B(t) > 0. \tag{14}$$

Cell capacitance is denoted by $C$. The relation between pack energy and internal power is simply given as

$$\dot{E}_B(t) = -P_B(t) \tag{15}$$

where standard sign convention has been adopted, indicating positive buffer power when discharging.

When scaling the electric buffer, it is assumed that the baseline number of cells $n_0$ is replaced with $n = s_B n_0$. It is interesting to note that buffer scaling does not explicitly affect (13) and (15). However, the physical limits on cell voltage and current

$$u(t) \leq u_{max}, \tag{16}$$

$$i_{min} \leq i(t) \leq i_{max}, \tag{17}$$

will be affected. This becomes evident when cell voltage is expressed by pack energy, and cell current by internal pack power and energy. Then, the limits can be written as

$$E_B(t) \leq s_B \frac{C u_{max}^2 n_0}{2}, \tag{18}$$

$$i_{min} \sqrt{\frac{2n_0}{C} E_B(t) s_B} \leq P_B(t) \leq i_{max} \sqrt{\frac{2n_0}{C} E_B(t) s_B}. \tag{19}$$

Recall that the square root function is concave in $E_B(t)$ and $s_B$, as a geometric mean of nonnegative variables. Hence, the constraint (19) preserves convexity, considering that $i_{min} \leq 0$, and $i_{max} \geq 0$.

Similar convex model can also be obtained for an electric battery, for which the cell open circuit voltage can be approximated as an affine function of state of charge. It turns out that such approximation is suitable for hybrid electric vehicle applications, where operation at too low and high state of charge is avoided due to battery longevity reasons. Further details on convex modeling of batteries can be found in Murgovski et al. (2012b); Egardt et al. (2014).

Table 3: Specifications for the supercapacitor cell.

| Parameter | Value[a] |
|---|---|
| Maximum open circuit voltage | $u_{max} = 2.85\,\mathrm{V}$ |
| Maximum discharging current | $i_{max} = 2200\,\mathrm{A}$ |
| Maximum charging current | $i_{min} = -2200\,\mathrm{A}$ |
| Internal resistance | $R = 0.29\,\mathrm{m\Omega}$ |
| Capacitance | $C = 3000\,\mathrm{F}$ |
| Mass[b] | $0.59\,\mathrm{kg}$ |

[a]BCAP3000 Maxwell cell. Available online: www.maxwell.com, December 2013.
[b]Includes 15 % additional mass for packaging and circuitry.

Supercapacitor cell specifications used in the example are given in Table 3.

*2.2.5. Objective function*

The optimization objective is formulated to minimize a cost function $\Phi(\cdot)$ consisting of operational and component cost. The operational cost is simply the cost for consumed hydrogen, and the components cost constitutes the cost for FCS and electric buffer. Then, the cost function can be written as

$$\Phi(\cdot) = w_h \int_0^{t_f} P_{Ff}(P_{Fe}(t), s_F)dt + w_F s_f + w_B s_B \tag{20}$$

where $w_h$, $w_F$, $w_B$ are weighting coefficients that transform the individual costs in currency/km, and $t_f$ is the time when the route is completed. The

weighting coefficients are computed as

$$w_h = \frac{c_h}{H_h d_{dc}}, \tag{21}$$

$$w_F = \frac{c_F P_{FeBmax}}{n_y d_y}\left(1 + p_y \frac{n_y + 1}{2}\right), \tag{22}$$

$$w_B = \frac{c_B n_0}{n_y d_y}\frac{C u_{max}^2}{2}\left(1 + p_y \frac{n_y + 1}{2}\right), \tag{23}$$

where $c_h$ is hydrogen price in currency/kg, $c_F$ is FCS price in currency/kW, $c_B$ is supercapacitor price in currency/kWh (including materials, manufacturing, packaging and circuitry), $H_h = 120\,\mathrm{MJ/kg}$ is lower heating value of hydrogen, $n_y$ is operational period of the bus, $d_y$ is yearly traveled distance of the bus, and $d_{dc}$ is length of the driving cycle, computed directly from the given velocity profile,

$$d_{dc} = \int_0^{t_f} v_{dem}(t)dt. \tag{24}$$

The expression $Cu_{max}^2/2$ in (23) indicates maximum energy of the supercapacitor cell, while terms in parentheses, in (22), (23), refer to depreciation expenses. It is assumed that there are no FCS and buffer replacements during the bus' operational period.

Description of the remaining parameters and values used in the example are given in Table 4.

*2.2.6. The convex optimization problem*

Finally, the optimization problem that has been formulated in Section 2.1, is translated here into mathematical language. A convex form of this problem is summarized in Table 5, where the problem has been written in a discrete form, using first order Euler discretization. It can be noticed that

Table 4: Parameter values used for computing weighting coefficients in the objective function.

| Parameter | Value |
|---|---|
| Hydrogen price[a] | $c_h = 4.44\,€/\text{kg}$ |
| FCS price[b] | $c_F = 34.78\,€/\text{kWh}$ |
| Supercapacitor price | $c_B = 10\,000\,€/\text{kWh}$ |
| Yearly travel distance | $d_y = 70\,000\,\text{km}$ |
| Bus' operational period | $n_y = 2\,\text{years}$ |
| Yearly interest rate | $p_y = 5\,\%$ |

[a]Swedish Gas Centre, Hulteberg and Aagesen (2009).

[b]Price for high-volume manufacturing, Spendelow and Marcinkoski (2012).

the mechanical and electrical torque/power balance constraints,

$$T_M(t) = T_0(t) + T_1(t)s_F + T_2(t)s_B + T_{brk}(t),$$
$$P_{Fe}(t) + P_B(t) - P_{Bd}(P_B(t), E_B(t)) - P_a = P_{Me}(T_M(t), t),$$

have been relaxed to

$$T_M(t) \geq T_0(t) + T_1(t)s_F + T_2(t)s_B, \tag{25}$$
$$P_{Fe}(t) + P_B(t) - P_{Bd}(P_B(t), E_B(t)) - P_a \geq P_{Me}(T_M(t), t). \tag{26}$$

The reason for relaxing (26) is needed to keep problem convexity, because in a convex optimization problem, the nonlinear terms, such as $P_{Bd}(P_B(t), E_B(t))$ and $P_{Me}(T_M(t), t)$, cannot be tied by an equality constraint. Although the relaxed problem is now different from the original problem, it is easy to argue that the optimal solution of the relaxed problem will be identical to the optimal solution of the original problem. The relaxation can be understood

Table 5: Pseudo code in CVX for convex optimization of simultaneous component sizing and energy management of a hybrid city bus.

minimize $w_h \sum_{k=1}^{N} \left( b_0 \boldsymbol{s_F} + b_1 \boldsymbol{P_{Fe}}(k) + b_2 \frac{\boldsymbol{P_{Fe}^2}(k)}{\boldsymbol{s_F}} \right) \Delta t + w_F \boldsymbol{s_f} + w_B \boldsymbol{s_B}$

with respect to: $\boldsymbol{P_{Fe}}(k), \boldsymbol{P_B}(k), \boldsymbol{E_B}(k), \boldsymbol{T_M}(k), \boldsymbol{s_F}, \boldsymbol{s_B}, \quad \forall k = 1, ..., N$

subject to:

$\boldsymbol{T_M}(k) \geq T_0(k) + T_1(k)\boldsymbol{s_F} + T_2(k)\boldsymbol{s_B},$

$\boldsymbol{P_{Fe}}(k) + \boldsymbol{P_B}(k) - \frac{RC}{2}\frac{\boldsymbol{P_B^2}(k)}{\boldsymbol{E_B}(k)} - P_a$

$\geq a_0(\omega_M(k)) + a_1(\omega_M(k))\boldsymbol{T_M}(k) + a_2(\omega_M(k))\boldsymbol{T_M^2}(k),$

$\boldsymbol{E_B}(k+1) - \boldsymbol{E_B}(k) = -\boldsymbol{P_B}(k)\Delta t,$

$\boldsymbol{E_B}(N+1) = \boldsymbol{E_B}(1),$

$\boldsymbol{T_M}(k) \geq T_{Mmin}(\omega_M(k)),$

$0 \leq \boldsymbol{P_{Fe}}(k) \leq \boldsymbol{s_F} P_{FeBmax},$

$0 < \boldsymbol{E_B}(k) \leq \boldsymbol{s_B}\frac{Cu_{max}^2 n_0}{2},$

$i_{min}\sqrt{\frac{2n_0}{C}\boldsymbol{E_B}(k)\boldsymbol{s_B}} \leq \boldsymbol{P_B}(k) \leq i_{max}\sqrt{\frac{2n_0}{C}\boldsymbol{E_B}(k)\boldsymbol{s_B}},$

$\boldsymbol{s_f} > 0,$

$\boldsymbol{s_B} > 0,$

for all $k = 1, ..., N.$

as letting the buffer throw away energy, which is certainly not optimal. The subsequent reasoning is that the constraint (26) must hold with equality for the optimal solution.

Similarly, the constraint (25) has been relaxed, by removing the braking torque from the problem. It is also evident that for a positive torque demand, the result where this constraint holds with inequality is not optimal, as this will mean delivering higher EM torque than demanded, which will trigger

unnecessary losses. When demanded torque is negative, however, this constraint may hold with inequality, if either the EM generating torque limit (8) is reached, or the buffer charging limit (19) is activated. The quantity that would satisfy this constraint with equality is exactly the braking torque, which can be obtained after the optimization is finished. A more rigorous proof that these relaxations will not change the properties of the optimal solution can be found in Egardt et al. (2014).

The convex problem has been written in CVX modeling language (Grant and Boyd, 2010), and solved with SeDuMi (Labit et al., 2002). A complete Matlab code is provided by Murgovski (2014). Optimization results are discussed in the following section.

### *2.3. Optimization results*

The correspondence between the total cost per kilometer and the sizes of the FCS and the buffer (i.e., the supercapacitor stack) is shown in Figure 6. It is indicated that the cost exhibits a complicated nonlinear relationship with respect to the sizes of power sources, rather than a simple monotonic interplay. However, it has been demonstrated that the convex programming is able to effectively find the global minimum (see the star in Figure 6). Additionally, the shaded area in Figure 6(b) reflects that some combinations of the sizes of FCS and electric buffer may lead to infeasible solutions that cannot meet the drivability requirements. The optimal cost, component sizes, and the computational time are summarized in Table 6.

The optimal power-split law between the FCS and the buffer, as well as the buffer SOC trajectory, is shown in Figure 7. It can be seen that the buffer provides relatively large transient power for effective FCS load leveling. The

Table 6: Optimization results.

| Parameter | Value |
|---|---|
| FCS size | 69.3 kW |
| Buffer size | 0.7 kWh |
| Total cost | 0.28 €/km |
| Computational time[a] | 10 s |

[a] 2.67 GHz dual-core processor was used with 4 GB RAM.

corresponding operational efficiencies of the FCS and the buffer are indicated in Figure 8. It is apparent that a majority of the operating points of the FCS and the buffer are located in high-efficiency area. Owing to a very low efficiency in the case of a relatively large power, the optimized buffer performs the power sinking/sourcing in a moderate manner.

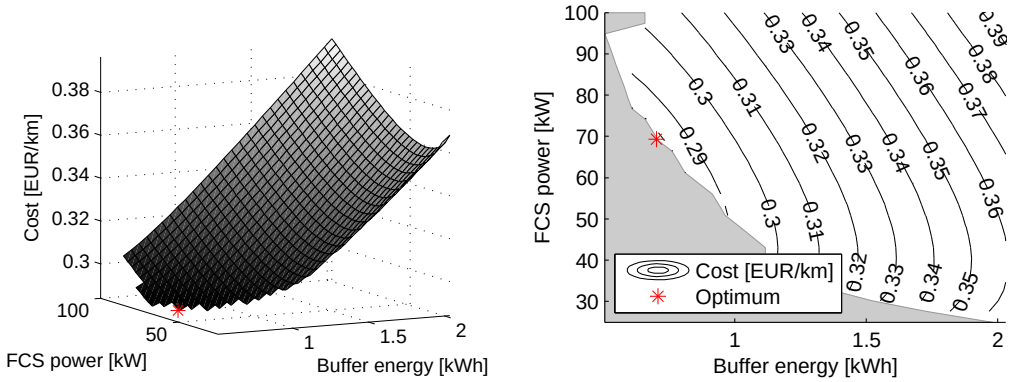


(a) Surface plot.

(b) Contour plot.

Figure 6: Optimal cost for different sizes of fuel cell system and electric buffer. The globally optimal solution is indicated by the star. The shaded region in (b) illustrates infeasible component sizes.

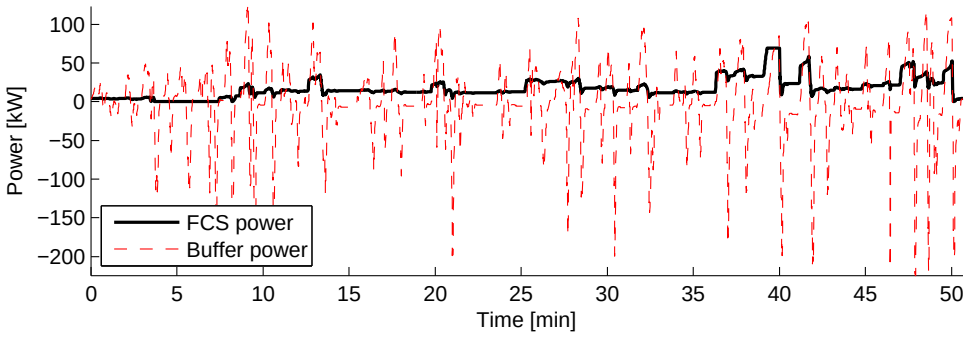


(a) Fuel cell system and electric buffer power trajectories.

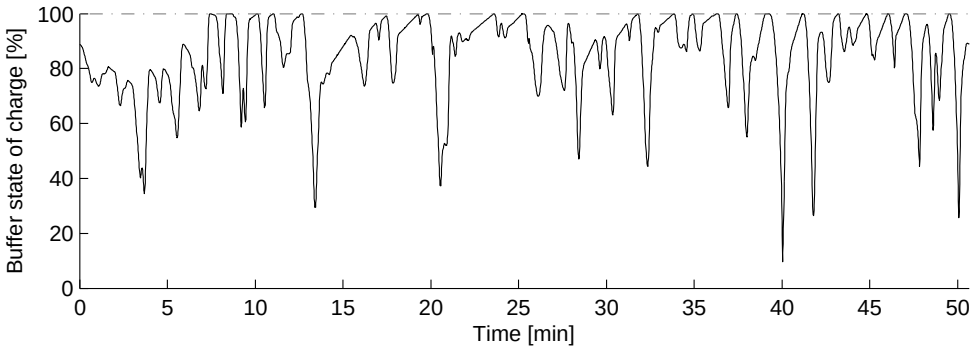


(b) State of charge of the electric buffer, computed as the ratio of operated and maximum supercapacitor voltage. The initial and final buffer charges are equal, thus conserving electric energy of the vehicle.

Figure 7: Optimal control and state trajectories.

## 3. Other powertrain configurations

In Section 2, a case study of a fuel cell/supercapacitor hybrid powertrain is introduced to illustrate the efficiency and fidelity of convex programming in a combined design and energy control optimization. Convex optimization, however, can also be applied to other powertrain configurations, such as parallel and series HEV powertrains, illustrated in Figure 9. In the parallel configuration, the ICE and the electric machine (EM) are mechanically cou-

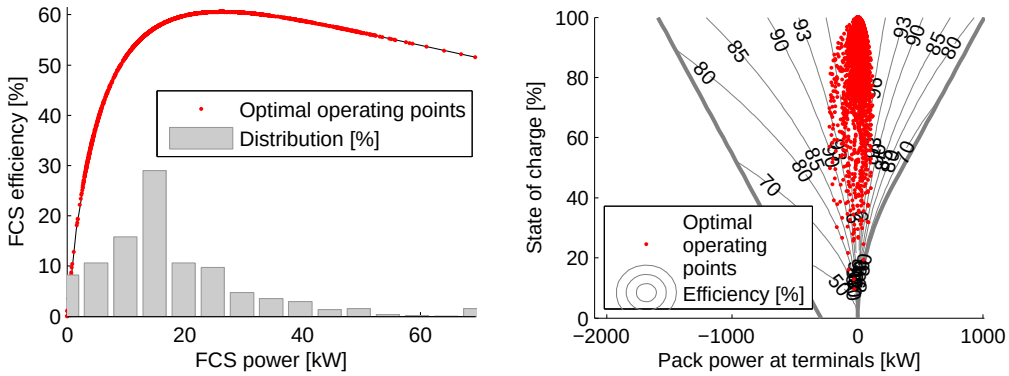


(a) Fuel cell system. Distribution of operating points is illustrated by the bars.

(b) Electric buffer. Power bounds are depicted by thick lines.

Figure 8: Optimal operating points of the fuel cell system and the electric buffer.

pled to the drive axle, so that the ICE is able to directly deliver mechanical energy to drive the wheels, in addition to a pure electric mode and a joint operation between the ICE and the EM. In contrast, the engine-generator unit (EGU), in the series configuration, is mechanically decoupled from the drive axle. In other words, there is no mechanical path delivering energy from the ICE. The ICE energy is first converted to electrical energy by means of the generator, and the electrical energy is then used to power the EM.

The key point for the convex modeling and optimization of the parallel HEV powertrain is approximation of fuel power as a convex function of the ICE net torque. A special case of describing fuel power as affine in torque, with speed dependent parameters, is known as Willans lines (Guzzella and Onder, 2010). Another common approximation, Guzzella and Sciarretta (2013); Murgovski et al. (2012c), describing fuel power as a quadratic function, similar to the approximated EM model in (7), has been illustrated in Figure 10(b). A detailed description of sizing and energy management of a

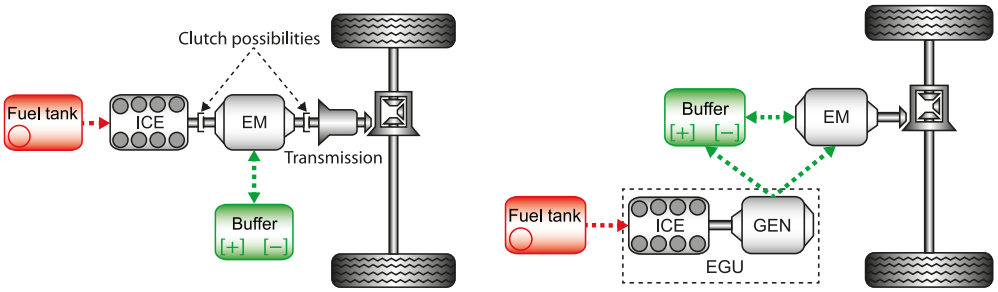


(a) Parallel hybrid electric powertrain. The engine (ICE) and electric machine (EM) are mechanically coupled to the drive axle.

(b) Series hybrid electric powertrain. The engine-generator unit (EGU) is mechanically decoupled from the drive axle.

Figure 9: Parallel and series hybrid electric powertrains. When EM operates as a motor, the electric energy flows from the buffer (battery or supercapacitor) to the wheels. When EM operates as a generator, the electric energy flows from the wheels, or ICE/EGU, to the buffer.

parallel hybrid electric vehicle, bus and a passenger car, via convex programming is detailed in Murgovski et al. (2012c); Pourabdollah et al. (2013).

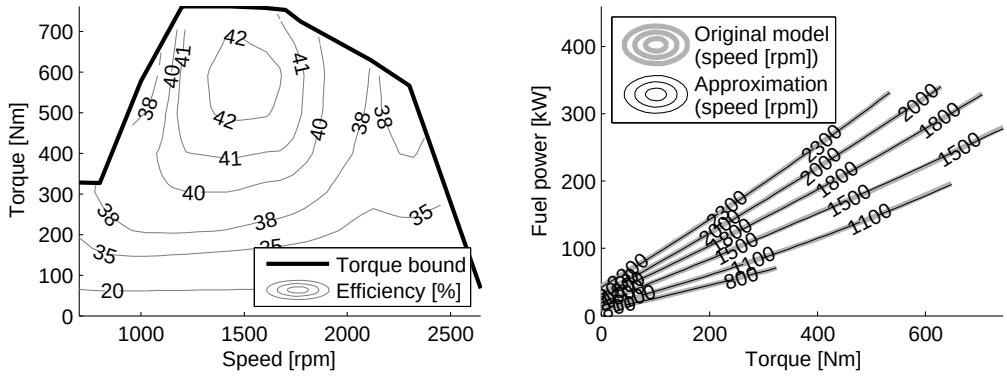


(a) Original model.

(b) Approximated model.

Figure 10: Quasi-static model of an internal combustion engine and its corresponding approximated model. The fuel power of the approximated model is quadratic in torque within the operating speed range of the engine.

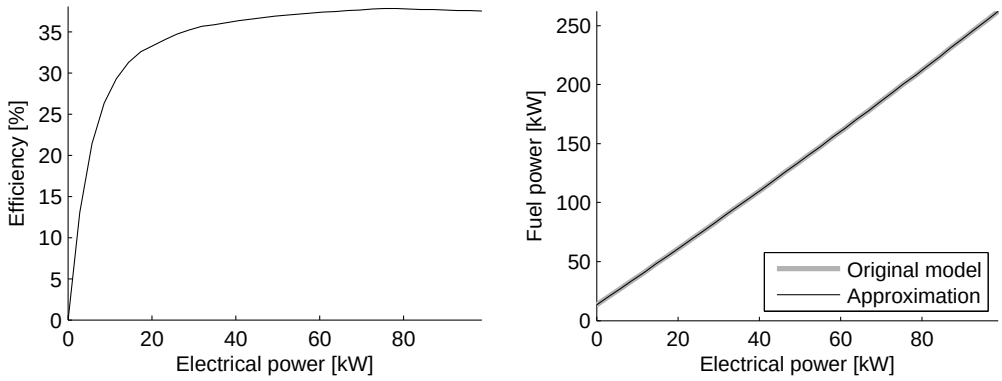


(a) Original model. (b) Approximated model.

Figure 11: Quasi-static model of an engine-generator unit (EGU) and its corresponding approximated model. The EGU is constructed from the electric machine and combustion engine illustrated previously, in Figure 4(a) and 10(a). The efficiency line is obtained by operating the engine and electric machine at the optimal operating points within the electrical power range of the EGU. The fuel power of the approximated model is quadratic in electrical power.

For the series powertrain, the challenge is to convexify the EGU. One well-established solution is to approximate the EGU by depicting the fuel power as a quadratic function of the generator net power. As illustrated in Figure 11, the quadratic EGU model can precisely describe real EGU energy loss. The tacit assumption behind the good approximation is that the EGU operates along the optimal operating line, which can be realized by a local EGU controller. A more thorough discussion on convex modeling and optimization of series hybrid electric vehicles is detailed in Murgovski et al. (2012c); Hu et al. (2013).

Besides the parallel and series configurations, convex optimization has also been extended to a series-parallel powertrain with a planetary gear as a

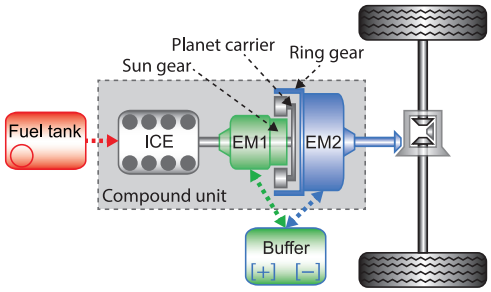


Figure 12: Series-parallel hybrid electric powertrain with a planetary gear as a power split device. The powertrain includes an internal combustion engine (ICE) and two electric machines, EM1 and EM2. The powertrain can be operated as a parallel HEV, when ICE and EM2 power the vehicle, or as a series HEV, when ICE and EM1 mimic an engine-generator unit.

power split device (see Figure 12). The strategy of convexifying the energy management problem relies on decomposing the problem into two optimization problems. The first is a static problem that looks for the optimal engine speed that maximizes efficiency of a compound unit, resembling an engine-generator unit combining the planetary gear and kinetic energy converters connected to it. The second is a dynamic optimization problem deciding the optimal power split between an electric buffer and the compound unit. By approximating the losses of the compound unit as convex, second order polynomial in electrical power, it is possible to solve the energy management problem using convex optimization (Murgovski et al., 2014a).

It is relevant to mention that integer decisions are often involved for the engine on/off and gearshift control in hybrid powertrains. As the set of integers is not convex, these signals have to be decided outside the convex program. One possible way to decide integer control signals is by using heuristics. Simple heuristic strategies that have been observed to give near optimal

results for series and parallel powertrains have been provided in Murgovski et al. (2012c); Pourabdollah et al. (2013). There are also more elaborate schemes that rely on iteratively solving a convex program. Strategies based on a synergy between convex optimization and Pontrygin's maximum principle are provided in Murgovski et al. (2013); Elbert et al. (2014).

A parallel HEV may also incorporate a continuous variable transmission, which allows replacing the gear shifting with a continuous speed ratio. This makes it possible to decide the optimal gear ratio by convex optimization, in which rotational energy of the part including the engine is now treated as a pure state variable. As a consequence, ICE's fuel power and EM's electrical power and torque constraints have to be expressed as convex functions of the rotational energy (or square of angular speed). Further details on this approach can be found in Murgovski et al. (2014b).

In addition to the supercapacitor stack discussed in Section 2.2.4, convex models for a battery pack and a dual buffer, combining both the battery and supercapacitor stacks, have been developed and integrated into the convex-optimization-based framework for component sizing and power management of hybrid electric powertrain (Hu et al., 2014). Moreover, the convex battery thermal and aging models have been also established in Murgovski et al. (2012a) and Murgovski et al. (2014b); Johannesson et al. (2013), respectively. Given these models, thermal or health-conscious sizing and energy control of hybrid powertrain via convex programming can be implemented. Interesting readers are referred to the related articles for further details.

## 4. Conclusion

In this chapter, the convex-programming framework for the combined design and control optimization of hybrid vehicles is described in a tutorial manner. The effectiveness and computational advantage of convex optimization is demonstrated, with the goal of encouraging more researchers and practitioners in the HEVs community to employ this useful tool for solving realistic optimization problems. An instructive case study of design and energy control optimization for a fuel cell/supercapacitor bus is straightforwardly presented, in which a pseudo code copy of CVX is also given to vividly and concretely elucidate practical implementation of convex optimization. The generalization, applicability, and validity of the convex-optimization framework are also discussed for diverse vehicular configurations (i.e., series, parallel, and series-parallel), different energy storage systems (e.g., battery, supercapacitor, and dual buffer), and advanced vehicular design and controller synthesis considering the battery thermal and aging conditions.

## Acknowledgment

This work was supported in part by the Swedish Energy Agency, Chalmers Energy Initiative and the Swedish Hybrid Vehicle Center.

## References

D. Assanis, G. Delagrammatikas, R. Fellini, Z. Filipi, J. Liedtke, N. Michelena, P. Papalambros, D. Reyes, D. Rosenbaum, A. Sales, and M. Sasena. An optimization approach to hybrid electric propulsion system design.

*Journal of Mechanics of Structures and Machines, Automotive Research Center Special Edition*, 27(4):393–421, 1999.

M. Back, M. Simons, F. Kirschbaum, and V. Krebs. Predictive control of drivetrains. In *Proc. IFAC World Congress*, Barcelona, Spain, 2002.

M. B. Beck, J. R. Ravetz, L. A. Mulkey, and T. O. Barnwell. On the problem of model validation for predictive exposure assessments. *Stochastic Hydrology and Hydraulics*, 11(3):229–254, June 1997.

D. Bertsekas and N. Sandell. Estimates of the duality gap for large-scale separable nonconvex optimization problems. In *21st IEEE Conference on Decision and Control*, volume 21, pages 782–785, 1982.

S. Boyd and L. Vandenberghe. *Convex Optimization*. Cambridge University Press, 2004.

A. J. Conejo, E. Castillo, R. Mnguez, and R. Garca-Bertrand. *Decomposition Techniques in Mathematical Programming. Engineering and science applications*. Berlin/Heidelberg/New York: Springer, 2006.

U. Eberle, B. Müller, and R. von Helmolt. Fuel cell electric vehicles and hydrogen infrastructure: status 2012. *Energy Environ. Sci.*, 5(10):8780–8798, 2012.

B. Egardt, N. Murgovski, M. Pourabdollah, and L. Johannesson. Electromobility studies based on convex optimization: Design and control issues regarding vehicle electrification. *IEEE Control Systems Magazine*, 34(2): 32–49, 2014.

P. Elbert, T. Nüesch, A. Ritter, N. Murgovski, and L. Guzzella. Engine on/off control for the energy management of a serial hybrid electric bus via convex optimization. *IEEE Transactions on Control Systems Technology*, 2014. Accepted with minor revisions.

H. Fathy, P. Papalambros, and A. Ulsoy. On combined plant and control optimization. In *8th Cairo University International Conference on Mechanical Design and Production*, Cairo University, 2004.

D. Feroldi, M. Serra, and J. Riera. Design and analysis of fuel-cell hybrid systems oriented to automotive applications. *IEEE Transactions on Vehicular Technology*, 58(9):4720–4729, 2009.

Z. Filipi, L. Louca, B. Daran, C.-C. Lin, U. Yildir, B. Wu, M. Kokkolaras, D. Assanis, H. Peng, P. Papalambros, J. Stein, D. Szkubiel, and R. Chapp. Combined optimisation of design and power management of the hydraulic hybrid propulsion systems for the 6 x 6 medium truck. *International Journal of Heavy Vehicle Systems*, 11(3):372–402, 2004.

R. Funck. *Handbook of Fuel Cells*. Hoboken, NJ: Wiley, 2003.

V. Galdi, L. Ippolito, A. Piccolo, and A. Vaccaro. A genetic-based methodology for hybrid electric vehicles sizing. *Soft Computing - A Fusion of Foundations, Methodologies and Applications*, 5(6):451–457, 2001.

F. Gasser. *An analytical, control-oriented state space model for a PEM fuel cell system*. PhD thesis, École Polytech. Fédérale de Lausanne, 2005.

M. Grant and S. Boyd. CVX: Matlab software for disciplined convex programming, version 1.21. `http://cvxr.com/cvx`, May 2010.

L. Guzzella and C. H. Onder. *Introduction to Modeling and Control of Internal Combustion Engine Systems*. Springer-Verlag, 2010.

L. Guzzella and A. Sciarretta. *Vehicle propulsion systems*. Springer, Verlag, Berlin, Heidelberg, 3 edition, 2013.

X. Hu, N. Murgovski, L. Johannesson, and B. Egardt. Energy efficiency analysis of a series plug-in hybrid electric bus with different energy management strategies and battery sizes. *Applied Energy*, 111(0):1001–1009, 2013.

X. Hu, N. Murgovski, L. Johannesson, and B. Egardt. Comparison of three electrochemical energy buffers applied to a hybrid bus powertrain with simultaneous optimal sizing and energy management. *IEEE Transactions on Intelligent Transportation Systems*, 2014. Accepted for publication.

C. Hulteberg and D. Aagesen. Hydrogen production for refueling applications. Technical Report SGC-R-210-SE, Swedish Gas Centre (SGC), 2009.

L. Johannesson, S. Pettersson, and B. Egardt. Predictive energy management of a 4QT series-parallel hybrid electric bus. *Control Engineering Practice*, 17(12):1440–1453, December 2009.

L. Johannesson, N. Murgovski, S. Ebbessen, B. Egardt, E. Gelso, and J. Hellgren. Including a battery state of health model in the HEV component sizing and optimal control problem. In *IFAC Symposium on Advances in Automotive Control*, Tokyo, Japan, 2013.

M. Kim and H. Peng. Power management and design optimization of fuel

cell/battery hybrid vehicles. *Journal of Power Sources*, 165(2):819–832, 2007.

M. Koot, J. T. B. A. Kessels, B. de Jager, W. P. M. H. Heemels, P. P. J. van den Bosch, and M. Steinbuch. Energy management strategies for vehicular electric power systems. *IEEE transactions on vehicular technology*, 54(3), May 2005.

Y. Labit, D. Peaucelle, and D. Henrion. SeDuMi interface 1.02: a tool for solving LMI problems with SeDuMi. *IEEE International Symposium on Computer Aided Control System Design Proceedings*, pages 272–277, September 2002.

V. Larsson, L. Johannesson, B. Egardt, and A. Lassson. Benefit of route recognition in energy management of plug-in hybrid electric vehicles. In *Proceeding of the 2012 American Control Conference*, June 2012.

J. Löfberg. YALMIP : A toolbox for modeling and optimization in Matlab. In *Proceedings of the CACSD Conference*, Taipei, Taiwan, 2004. URL `http://users.isy.liu.se/johanl/yalmip`.

R. Mnguez, A. J. Conejo, and E. Castillo. Optimal engineering design via Benders' decomposition. *Annals of Operations Research*, 210(1):273–293, 2013. ISSN 0254-5330.

N. Murgovski. *Optimal Powertrain Dimensioning and Potential Assessment of Hybrid Electric Vehicles*. PhD thesis, Chalmers University of Technology, Gothenburg, Sweden, 2012.

N. Murgovski. CONES: Matlab code for convex optimization in electromobility studies. `https://publications.lib.chalmers.se/publication/192858`, January 2014.

N. Murgovski, L. Johannesson, J. Hellgren, B. Egardt, and J. Sjöberg. Convex optimization of charging infrastructure design and component sizing of a plug-in series HEV powertrain. In *IFAC World Congress*, Milan, Italy, 2011.

N. Murgovski, L. Johannesson, A. Grauers, and J. Sjöberg. Dimensioning and control of a thermally constrained double buffer plug-in HEV powertrain. In *51st IEEE Conference on Decision and Control*, Maui, Hawaii, December 10-13 2012a.

N. Murgovski, L. Johannesson, and J. Sjöberg. Convex modeling of energy buffers in power control applications. In *IFAC Workshop on Engine and Powertrain Control, Simulation and Modeling (E-CoSM)*, Rueil-Malmaison, Paris, France, October 23-25 2012b.

N. Murgovski, L. Johannesson, J. Sjöberg, and B. Egardt. Component sizing of a plug-in hybrid electric powertrain via convex optimization. *Mechatronics*, 22(1):106–120, 2012c.

N. Murgovski, L. Johannesson, and J. Sjöberg. Engine on/off control for dimensioning hybrid electric powertrains via convex optimization. *IEEE Transactions on Vehicular Technology*, 62(7):2949–2962, 2013.

N. Murgovski, X. Hu, and B. Egardt. Computationally efficient energy management of a planetary gear hybrid electric vehicle. In *IFAC World Congress*, Cape Town, South Africa, 2014a.

N. Murgovski, L. Johannesson, and B. Egardt. Optimal battery dimensioning and control of a CVT PHEV powertrain. *IEEE Transactions on Vehicular Technology*, 63(5):2151–2161, 2014b.

D. L. Peters, P. Y. Papalambros, and A. G. Ulsoy. Sequential co-design of an artifact and its controller via control proxy functions. *Mechatronics*, 23 (4):409–418, 2013.

M. Pourabdollah, N. Murgovski, A. Grauers, and B. Egardt. Optimal sizing of a parallel PHEV powertrain. *IEEE Transactions on Vehicular Technology*, 62(6):2469–2480, 2013.

J. A. Reyer and P. Y. Papalambros. Combined optimal design and control with application to an electric dc motor. *Journal of Mechanical Design*, 142(2):183–191, 2002.

A. Sciarretta and L. Guzzella. Control of hybrid electric vehicles. *IEEE Control Systems Magazine*, 27(2):60–70, April 2007.

J. Spendelow and J. Marcinkoski. Fuel cell system cost-2012. DOE fuel cell technologies program record. Technical Report 12020, US Department of Energy, 2012.

O. Sundström, L. Guzzella, and P. Soltic. Torque-assist hybrid electric powertrain sizing: From optimal control towards a sizing law. *IEEE Transactions on Control Systems Technology*, 18(4):837–849, July 2010.

E. D. Tate and S. P. Boyd. Finding ultimate limits of performance for hybrid electric vehicles. In *SAE Technical Paper 2000-01-3099*, 2000.

E. Tazelaar, Y. Shen, P. Veenhuizen, T. Hofman, and P. van den Bosch. Sizing stack and battery of a fuel cell hybrid distribution truck. *Oil & Gas Science and Technology - Rev. IFP Energies nouvelles*, 67(4):563–573, 2012a.

E. Tazelaar, B. Veenhuizen, P. van den Bosch, and M. Grimminck. Analytical solution of the energy management for fuel cell hybrid propulsion systems. *IEEE Transactions on Vehicular Technology*, 61(5):1986–1998, 2012b.

S. Terwen, M. Back, and V. Krebs. Predictive powertrain control for heavy duty trucks. In *Proc. IFAC Symposium on Advances in Automotive Control*, Salerno, Italy, 2004.

K. C. Toh, R. H. Tütüncü, and M. J. Todd. On the implementation and usage of SDPT3 - a Matlab software package for semidefinite-quadratic-linear programming, version 4.0, July 2006.

TOSA. Tosa flash mobility, clean city smart bus. http://www.tosa2013.com/, 2013.

Volvo Group. Volvo 7900 Hybrid Bus. http://www.volvo.com, 2013.

L. Wu, Y. Wang, X. Yuan, and Z. Chen. Multiobjective optimization of HEV fuel economy and emissions using the self-adaptive differential evolution algorithm. *IEEE Transactions on Vehicular Technology*, 60(6):2458–2470, 2011.

L. Xu, J. Li, J. Hua, X. Li, and M. Ouyang. Adaptive supervisory control strategy of a fuel cell/battery-powered city bus. *Journal of Power Sources*, 194(1):360–368, 2009.

## Appendix A. Convex optimization

A standard notation for a convex problem is defined as follows

$$\begin{aligned} &\text{minimize} && f_0(x) \\ &\text{subject to} && f_i(x) \leq 0, \quad i = 1, ..., m \\ &&& h_i(x) = 0, \quad i = 1, ..., p \end{aligned} \tag{A.1}$$

where $x \in \mathbb{R}^n$ is a vector of optimization variables, $h_i(x), i = 1, ..., p$ are affine functions in $x$, and $f_j(x), j = 0, ..., m$ are convex functions. A function $f : \mathbb{R}^n \to \mathbb{R}$ is convex if $\operatorname{dom} f$ is a convex set and

$$f(\theta x + (1 - \theta)y) \leq \theta f(x) + (1 - \theta)f(y) \tag{A.2}$$

for all $x, y \in \operatorname{dom} f$ and any $\theta$ with $0 \leq \theta \leq 1$. Or, in other words, the line segment between any two points on the graph of a convex function lies above the graph (see Figure A.13 for illustration). In the notation above, $\operatorname{dom} f$ stands for domain of $f$ and the set of real numbers is denoted by $\mathbb{R}$.

Convex optimization problems have two important properties. First, any obtained optimal solution is also globally optimal. Second, the problem can be solved, very reliably and efficiently, using interior-point methods or other special methods for convex optimization. There are also generally available solvers, e.g. SeDuMi (Labit et al., 2002) and SDPT3 (Toh et al., 2006), and higher level optimization modeling languages such as CVX (Grant and Boyd, 2010) and YALMIP (Löfberg, 2004).

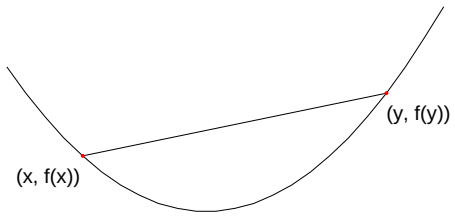


Figure A.13: Graph of a convex function. The line segment between any two points on the graph lies above the graph.

Assertion of convexity of the optimization problem studied in this chapter follows directly from definition (A.1) and some properties of convex functions, which read as follows:

- The function $f$ is said to be concave if $-f$ is convex.
- An affine function $h(x) = qx + r$ is both convex and concave.
- A quadratic function $f(x) = px^2 + qx + r$ with $\mathrm{dom}\, f \subseteq \mathbb{R}$ is convex if $p \geq 0$.
- A quadratic-over-linear function $f(x, y) = x^2/y$ with $\mathrm{dom}\, f = \{(x, y) \in \mathbb{R}^2 \,|\, y > 0\}$ is convex.
- The geometric mean $f(x, y) = \sqrt{xy}$ with $\mathrm{dom}\, f = \{(x, y) \in \mathbb{R}^2 \,|\, x, y \geq 0\}$ is concave.
- A nonnegative weighted sum $f = \sum w_i f_i$ with $w_i \geq 0$, of convex functions $f_i$, is a convex function.
- *A product $f(x, y) = x\, y$ is generally not a convex function.*

For further details on convex optimization and applications, readers are referred to Boyd and Vandenberghe (2004).